



Treball Final de Grau

Characterization of industrial membranes by imaging and chemometrics.

Caracterización de membranas industriales mediante imágenes y quimiometría.

Laia Vanacloy Garcia

January, 2020



Aquesta obra esta subjecta a la llicència de:
Reconeixement–NoComercial–SenseObraDerivada



<http://creativecommons.org/licenses/by-nc-nd/3.0/es/>

En este último trabajo de esta etapa tan importante para mí, he de agradecer a Rodrigo por haberme ayudado y enseñado los conocimientos que he aplicado en este trabajo. A demás agradecerle tanto a él como a Adri y Betta por ser unos compañeros geniales y hacer de las horas de trabajo unos muy buenos momentos y guardar muy buenos recuerdos de este trabajo. Por supuesto agradecer a Anna, mi tutora, por todo el tiempo invertido para hacer posible este trabajo y hacerme sentir una más del grupo.

Por último, pero no menos importante, dar las gracias a mi familia y amigos por estar durante esta etapa de estrés y nervios apoyándome y confiando en mí.

A todos ellos, muchas gracias.

REPORT

CONTENTS

1. SUMMARY	3
2. RESUMEN	5
3. INTRODUCTION	7
3.1. Industrial use of membranes	7
3.2. Types of ionic exchange membranes	8
3.3 Analytical techniques for membrane characterization	8
3.3.1. Single-point spectroscopy	9
3.3.1.1. NIR	9
3.3.1.2. Mid-IR	9
3.3.2. Hyperspectral imaging	11
3.3.2.1. NIR images	12
3.3.2.2. Mid-IR images	12
4. OBJECTIVES	13
5. EXPERIMENTAL SECTION	13
5.1. Sample description	13
5.2. Sample preparation	15
5.3 Instrumental measurements	17
5.3.1. Single-point spectra	18
5.3.2. Hyperspectral images	18
6. DATA TREATMENT	20
6.1. Spectra preprocessing	20
6.2. Multivariate Curve Resolution-Alternating Least Squares (MCR-ALS)	22
7. RESULTS AND DISCUSSION	25
7.1. Optical characterization of membranes	25
7.2. Single-point spectroscopy of membranes	27
7.3 Hyperspectral images	30
7.3.1. Mid-IR images	30
7.3.2. NIR hyperspectral images	34
8. CONCLUSIONS	37
9. REFERENCES AND NOTES	39

1. SUMMARY

In the last years the use of membranes in the industry has increased significantly. Among the types of membranes used, there exist the ionic exchange membranes, which are used in many cases, such as the production of wine and the valorisation of acidic liquid wastes. During their usage, it is possible to have an accumulation of solid material on the surface of the membranes known as fouling.

The physicochemical characterization of the membranes and the fouling is very important to understand and improve the performance of membranes in industrial processes. For that reason, the potential of mid-Infrared (mid-IR) and Near Infrared (NIR) spectroscopy was tested in the characterization of two commercial membranes, Fujifilm and Neosepta, by using single-point spectroscopy and hyperspectral images. The spectroscopic measurements were done in reflectance mode to characterize the surface of the membranes, and in transmission mode, to characterize the membrane cross-section and obtain information about the composition of the fouling and the membrane. In the case of hyperspectral images, the chemometric method Multivariate Curve Resolution-Alternating Least Squares (MCR-ALS) was used to interpret the data and to obtain information about the composition and spatial structure of the fouling and membrane components.

Finally, it has been demonstrated that the determination of the composition and the distribution of the components of the membranes is possible combining spectroscopic techniques with the suitable chemometric tools. For each membrane studied, the right characterization was done with a different technique (NIR for Neosepta and mid-IR for Fujifilm) due to the natural characteristics of the membranes and their fouling.

Keywords: industrial membranes, hyperspectral images, Chemometrics, Near infrared (NIR) spectroscopy, Mid-infrared (mid-IR) spectroscopy.

2. RESUMEN

En los últimos años el uso de membranas en la industria ha aumentado notablemente. Entre estas membranas existen las llamadas de intercambio iónico que son utilizadas en procesos como la producción del vino o la depuración de aguas ácidas. Durante su uso es posible que en su superficie se dé la acumulación de materia sólida que es lo que se conoce como *fouling*.

La caracterización no solo de la membrana en sí sino también del *fouling* formado es de gran importancia para comprender y mejorar el funcionamiento de las membranas en procesos industriales. Por ese motivo en este trabajo se estudió el potencial de las espectroscopías de infrarrojo medio (mid-IR) e infrarrojo cercano (NIR) para la caracterización de dos membranas comerciales, Fujifilm y Neosepta, mediante mediciones de espectros puntuales y de imágenes hiperespectrales. Ambas mediciones se realizaron utilizando el modo de reflectancia, para la caracterización exclusiva de la superficie de las membranas, y el modo de transmisión, para la caracterización de la sección transversal de la membrana, que proporciona información tanto de la composición del *fouling* como de la membrana. En el caso de las imágenes hiperespectrales se utilizó el método quimiométrico de resolución multivariante de curvas por mínimos cuadrados alternados (MCR-ALS) para interpretar los datos y obtener información sobre la composición y estructura espacial de las membranas.

Finalmente, se ha podido demostrar que es posible determinar la composición y la distribución de los componentes que tienen ambas membranas, combinando las técnicas espectroscópicas estudiadas con las herramientas adecuadas que proporciona la quimiometría. La caracterización de cada membrana se ha llevado a cabo correctamente con técnicas diferentes (mid-IR para Fujifilm y NIR para Neosepta), debido a la naturaleza diferente tanto de su composición como del *fouling* que presentan.

Palabras clave: membranas industriales, imágenes hiperespectrales, Quimiometría, espectroscopia de infrarrojo cercano (NIR), espectroscopia de infrarrojo medio (Mid-IR).

3. INTRODUCTION

3.1. INDUSTRIAL USE OF MEMBRANES

In the last years the use of membranes in the industry has increased. These membranes are used in a process of filtration where the membrane separates the liquid part from the solid on suspension in the solution. One of the most common uses of the membranes is the filtration and depuration of water, but nowadays they are used too in alimentary and pharmaceutical industries. Besides, membranes allow selective separation processes, where liquid phases in both sides of the membrane have different composition. Membranes separate two liquid phases, permeate and retentate, with different compositions. On one side, particles, colloids or macromolecules can be retained, for instance. Depending on the type of the membrane, some ions or molecules can be favoured to pass from one side of the membrane to the other. In general, membranes allow separation processes in sustainable conditions because no heating or big apportionment of energy is required.

The way that the membranes work is based in the fact that the membranes act as a specific filter where the initial liquid phase will go through with certain molecules and ions incorporated, while the solid phase will be retained in the surface of the membrane and the retained liquid phase will present a different composition, which means that the membrane works as a selective barrier. To make possible that the solution passes through the membrane different methods exist for example the application of high pressure or the introduction of an electric potential. These methods adapt to the membrane separation mechanism.

Since the solid that was in suspension in the initial solution is collected on the surface of the membrane it is necessary to do the characterization of this material, called fouling, to know what exactly that suspension was and how the fouling can affect the structure and operation of the membrane. To do this is necessary to characterize the clean membrane too, so it will be possible to compare both compositions and structures and find the differences, because it is very possible that the fouled part affects the membrane.

Within the membranes that are used in the industry, we can mention different types: reverse osmosis, nanofiltration, ultrafiltration, microfiltration and ionic exchange membranes. In this work the membranes that were used were the ionic exchange ones so for this reason this type of membranes will be further explained.

3.2. TYPES OF IONIC EXCHANGE MEMBRANES

An ionic exchange membrane transports certain dissolved ions, while blocking other ions or neutral molecules. The ionic exchange membranes (IEM) are formed by a hydrophobic substrate, an immobilized ion-functionalized group and a movable counter-ion. Their structure is formed by nets of nanofibers of polymers and between these nanofibers there are gaps that are filled with the ion-exchange aliphatic polymer. These membranes work based on the interaction of the ionic groups of the membrane and the ions in the process solution. The membrane in contact with the process solution will allow ions of the opposite charge to pass through the membrane, while blocking ions with charge of the same sign, see figure 1 ^{1,2}.

According to the ionic group that the membrane has the IEM's can be classified in anionic exchange membranes (AEM), which let anions to pass through, or cationic exchange membranes (CEM), which let cations to pass through.

In the case of the AEM's the common cationic groups used to fill the gaps in the fibres are quaternary ammonium bases ($-(\text{CH}_3)_3\text{N}^+$), imidazole cations ($-\text{C}_3\text{H}_5\text{N}_2^+$) and guanidium cations ($-\text{C}(\text{NH}_2)_3^+$).

For the CEM's the common anionic groups used to fill the space between the fibres are sulfonic groups ($-\text{SO}_3^-$), phosphoric groups ($-\text{PO}_4^{3-}$) and carboxylate groups ($-\text{COO}^-$).

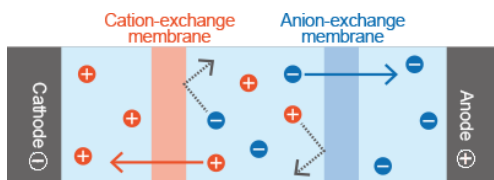


Figure 1. Illustration of how IEM's work. Image extracted from <https://www.fujifilm.com/innovation/technologies/separation-of-gases-or-liquids/> (last access January 2020).

3.3. ANALYTICAL TECHNIQUES FOR MEMBRANE CHARACTERIZATION

To do the characterization of the membranes, different types of spectroscopic techniques, such as near infrared (NIR) and mid infrared (Mid-IR) can be used. In the Mid-IR, there exist different spectroscopic modes to do the membrane characterization, such as Attenuated Total Reflectance (ATR) or transmission. In NIR, the membrane characterization is done in

reflectance mode. Both NIR and Mid-IR spectroscopy techniques can be used to acquire a single spectrum of the sample or a full hyperspectral image.

3.3.1. Single-point spectroscopy

Punctual spectra give information about the composition of a specific point of the sample. This measurement is useful when the sample has visible different zones. The single-point spectra can be collected using a reflectance or a transmission mode. The difference between the two modes besides the fundamentals, is that in the reflectance mode the thickness of the sample is not important while in the transmission mode if the sample is too thick the measurement could not be done.

3.3.1.1. NIR

NIR spectroscopy works in the region of wave-numbers of $\sim 4000\text{-}13000\text{ cm}^{-1}$ in the electromagnetic spectrum. The absorption in this region of the spectrum is due to overtones and combination of vibrational fundamental bands of molecular vibrations that take place in the range of $3000\text{-}1700\text{ cm}^{-1}$. The most important bonds that absorb in this region are the ones involving hydrogen, such as C-H, N-H and O-H bonds³.

To obtain spectra in NIR it is used the reflectance mode, which consists of measuring the radiation reflected by the sample surface after applying a beam of IR light, see figure 2. The most usual samples that are measured in reflectance mode are thick solid samples. Since the reflectance measures the sample surface, the thickness of the sample is not important.

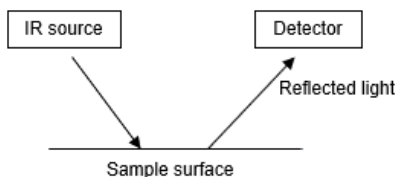


Figure 2. Illustration of how reflectance mode works.

3.3.1.2. Mid-IR

Mid-IR spectroscopy corresponds to the region of wavenumbers of $\sim 400\text{-}4000\text{ cm}^{-1}$ in the electromagnetic spectrum. The absorption in this region corresponds to the fundamental bands of molecular vibrations and provides a molecular finger print. In comparison with the spectra in

the NIR region, the ones in the Mid-IR are clearer because they are not formed by combination bands, as the NIR ones ⁴. Mid-IR spectroscopy can be used in different spectrometric modes, such as ATR or transmission mode.

The ATR measures the surface of the sample, what means that it works in reflectance mode, as NIR. The sample in this technique must be in contact with the part known as ATR crystal. Once the sample is in the right position, a beam of infrared light travels through the crystal and enters in contact with the sample. That beam reflects and forms an evanescent wave that extends into the sample. The interaction of the IR beam and the sample happens through the evanescent wave, see figure 3. The beam is absorbed according to the composition of the sample and the final IR light reflected does not have the absorbed parts and it is attenuated; hence the name of the technique, Attenuated Total Reflection ⁵.

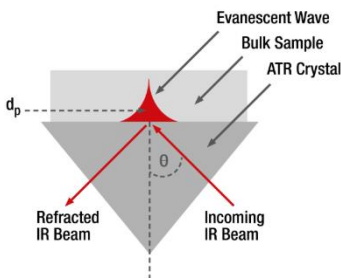


Figure 3. Scheme of how ATR works. Extracted from <https://wiki.anton-paar.com/en/attenuated-total-reflectance-atr/> (last access 2020).

The other mode that can be used in measurements with Mid-IR spectroscopy is the transmission mode, in which the IR light goes through the sample ⁶. The light with a specific wavelength will be absorbed by the sample, the light that has not been absorbed goes through the sample and is collected by the detector, see figure 4. Since in this mode the light goes through the sample, it is necessary to take care of the thickness of the sample, because if it is too thick the measure is not possible. Another thing that is necessary to keep in mind when the transmission measurements are done is where the sample is placed. Normally CaF_2 slides, which are transparent in the IR spectral range and would not affect to the spectrum, are used. For this reason, the transmission mode measurements of the membranes are done on cross-section cuts, which are thin enough for this mode.

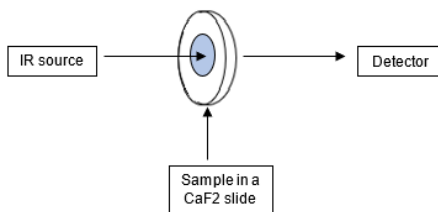


Figure 4. Scheme of transmission mode working procedure in FT-IR spectroscopy.

The conventional IR light beam covers a field of view of 20 μm , but it can also be used the synchrotron beam, which is a very bright and collimated source that makes possible to have more spatial resolution reaching a field of view of 3 μm .

3.3.2. Hyperspectral imaging

Hyperspectral imaging includes all kinds of spectroscopic systems that allow acquiring a chemical image, where every pixel is associated with a full spectrum. All spectra in a hyperspectral image are organized to form a cube of data, with two spatial dimensions (x- and y-) and one spectral dimension that will be analysed to have information about the composition of samples, see figure 5. Hyperspectral images give spatial and spectral information about the samples. The objective is to obtain information about the composition of samples, which means to know which components form the samples and where they are located. To do the analysis of the big number of spectra in the image cube, it is necessary to use chemometrics to do the interpretation of the initial information obtained, as will be explained in the next section.

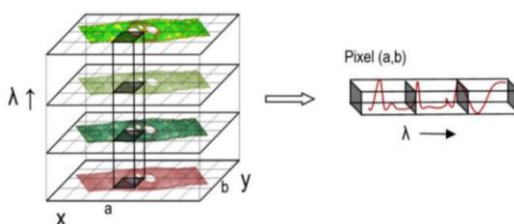


Figure 5. Illustration of a hyperspectral image. On the left an image cube with the spatial coordinates x and y, and λ as the spectral coordinate. On the right the representation of a pixel with its corresponding spectrum formed with several responses at different wavelengths.

3.3.2.1. NIR images

The NIR images are obtained in reflectance mode, which means that the signal collected corresponds to the light reflected by the sample. Therefore, the images that are done with NIR are from the membrane surface. As in the case of the single-point spectra, the thickness of the sample in reflectance mode is not relevant, that is why the NIR images obtained are from the membrane surface without any treatment.

3.3.2.2. Mid-IR images

The system used to do Mid-IR hyperspectral images is using an infrared imaging microscope as instrument. This instrument works in transmission mode, which means that the IR beam goes through the sample. For this reason, as in single-point spectroscopy, it is necessary to take care of the thickness of the sample. These images are used to analyse samples of cross-section of the membranes that have a few μm of thickness.

This instrument has four different components: the first one is the IR light source. The second component is formed by the beam splitters and filters whose utility is for focus in the different wavelengths. The third component is a detector that will collect and record the signal that the sample gives. Finally, the last component is an optical microscope that makes possible to acquire the infrared image related to the sample ^{7,8}, see figure 6.

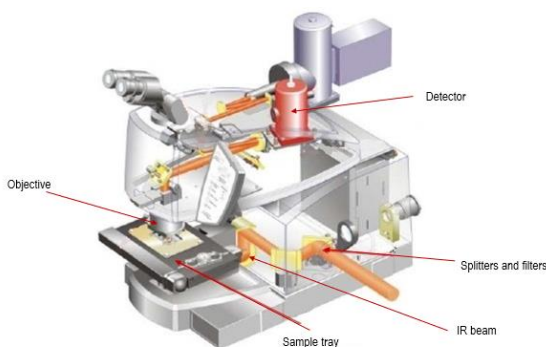


Figure 6. Illustration of a microscope. Extracted from <https://pt.slideshare.net/atahualpacordero/ftir-politcnica-charla-de-espectroscopia-infrarroja-por-transformadas-de-fourier/24?smtNoRedir=1> (last access: January 2020).

4. OBJECTIVES

The objective of this work is to propose an analytical protocol including spectroscopic measurements in the mid-infrared (mid-IR) and the near infrared (NIR) range and related chemometric analysis for the characterization of membranes, used in industrial processes, and the fouling that can be deposited on them during their use. In this study, two ion-exchange membranes were taken as examples to be characterized: the Fujifilm membrane, which was used in the production of wine, and the Neosepta membrane, which was used in the valorisation of acidic liquid wastes.

To achieve this general objective, it is necessary to perform the following tasks:

- Optimization of the sample treatment (drying, embedding, sectioning) when the measurements need to be done on membrane cross-sections.
- Testing of all possible mid-IR and NIR measurements to obtain information on the membranes. This includes doing the characterization by single-point spectra to know the composition of specific points in the membrane and by hyperspectral images to know the spatial distribution of these components in the membrane. Both NIR and Mid-IR spectroscopies are also tested working in reflectance mode (to study the membrane surface) and in transmission mode (to study membrane cross-sections).
- Optimizing the chemometric data treatment to make possible the characterization of the composition and spatial distribution of the components that each membrane has.

5. EXPERIMENTAL SECTION

5.1. SAMPLE DESCRIPTION

We worked with two different anionic exchange membranes (AEM), one provided by Fujifilm and another one by Astom.

The Fujifilm membrane is an AEM type II and has a structure of disordered polyolefin nanofibers, formed by an electrospinning method. This structure has spaces between the fibres

that are filled with aliphatic polyamide (PA) functionalized by quaternary ammonium bases – $(\text{CH}_3)_3\text{N}^+$. This latter component makes possible the anionic exchange ¹.

This membrane has a thickness of 0.16 mm, an electrical resistance of $8 \Omega \text{ cm}^2$, a perm selectivity described by the IUPAC ⁹ as “a term used to define the preferential permeation of certain ionic species through ion-exchange membranes” of 96 (measured at 0.05-0.5 M NaCl), a burst strength, which is the pressure at which the membrane will burst, used as a measure of the resistance to rupture, of 4.7 kg/cm^2 and pH stability between 2-10 ¹⁰.

The Fujifilm membrane was used in the industry of wine. The objective of this membrane is allowing the pass through of anions of hydrogen tartrate (TH^-) that are found in the untreated wine ¹¹. On the other hand, the cations go through the cationic exchange membranes (CEM) and end in the same solution as the (TH^-). The solution with the ions of TH^- and the cations is collected to recover the TH^- , meanwhile the treated wine, low in TH^- and cations, is collected too, see figure 7. The fouling that the membrane has is mainly due the accumulation of polyphenols and polysaccharides.

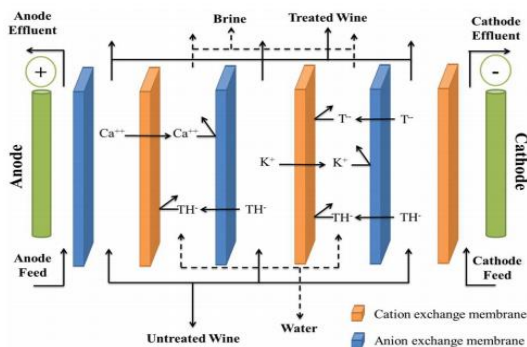


Figure 7. Representation of the use of the Fujifilm membrane. (Image extracted from Membrane Technologies in Wine Industry: An Overview. ref. 11).

The Astom membrane is a Neospeta and has a structure of a polyvinyl chloride fabric (PVC) with a mixture of polystyrene and divinylbenzene functionalized with the same ion exchange material as in the Fujifilm membrane ¹.

This membrane has a thickness of 0.17 mm, an electrical resistance of $1 \Omega \text{ cm}^2$ (measured at 0.05-0.5 M NaCl), a burst strength of 0.15 MPa and pH stability between 0-8 ¹².

The Neosepta membrane was used for the valorisation of acidic liquid wastes ¹³. In this process the objective is recovering the sulfuric acid that the solution has. The HSO_4^- and SO_4^{2-} anions pass through the membrane and are collected in water to make possible the reuse of the sulfuric acid. The cations with positive charge will stay in the initial solution, see figure 8. In this case the composition of the fouling in the membrane surface is not exactly known, but probably is molecular sulphur.

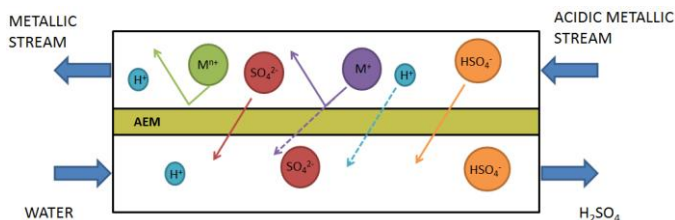


Figure 8. Representation of the use of the Neosepta membrane. (Extracted from the PhD thesis of Julio López Rodríguez, ref. 13).

5.2. SAMPLE PREPARATION

The surface membrane measurements did not need any pretreatment of the sample.

To obtain membrane cross-sections it was necessary to make a treatment of the sample that consisted of drying the sample, doing an embedding with paraffin of the membranes and cutting the embedded sample in cross-sections of some μm of thickness. The samples of the fouled Fujifilm membrane were dried in different ways to see if there was any difference in the spectral measurements due to the way that the sample was dried. Before making any of these drying treatments the Fujifilm membrane was cut in three strips of 3 mm width, to test the three different drying treatments. One of the treatments consisted of letting one strip dry overnight in a desiccator at room temperature. (FuS1).

The second one consisted of a dehydration of the strip by doing sequential 10 min immersions in ethanol, first with ethanol 50% (v/v), then 70%, 80%, 90% and finally 100%. (These solutions were made with ethanol 99.98% and water) ¹⁴. After the immersions were done the membrane was let drying overnight in a desiccator at room temperature. (FuS2).

For the last treatment the same dehydration process as in FuS2 was made, but after that, the sample was kept in a solution of ethanol 100% overnight. The next day the sample was treated doing two 10 min immersions in xylol. (FuS3).

In the case of the new Fujifilm membrane, the strips done were: one for the new Fujifilm kept in brine (FB), one of the Fujifilm kept without any treatment (F). For the Neosepta membrane, one strip was of the fouling part of the Neosepta membrane (NF) and one of the part of the Neosepta that have fouling and clean membrane (NFC). The only treatment that was made to these samples was leaving the strips overnight in the desiccator at room temperature.

The embedding of the samples consisted of putting a piece of the sample with liquid paraffin in a mould, that was left in an oven at 56°C for an hour or overnight. After that the mould was left with ice blocks to get the piece of solid paraffin with the sample in it.

Once the samples were embedded, the last step to have the samples in the correct way to perform measurements in transmission mode was making cross-sections of 5 and/or 10 μm thickness with the Leica Rm 2135 microtome, located at the Parc Científic of Barcelona, and placing them between slides of CaF_2 . All drying and embedding procedures for the membrane cross-sections are summarized in table 1.

Table 1. Codes of all the dried and embedded samples.

Sample code	Membrane	Drying	Section thickness
FuS1	Fujifilm + fouling	Overnight at room temperature.	5 and 10 μm
FuS2	Fujifilm + fouling	Sequential immersions in EtOH + overnight at room temperature.	5 and 10 μm
FuS3	Fujifilm + fouling	Sequential immersions in EtOH + EtOH 100%(v/v) overnight + xylol	5 and 10 μm
FB	Fujifilm new kept in brine	Overnight at room temperature.	5 and 10 μm
F	Fujifilm new	Overnight at room temperature.	--
FC	Fujifilm clean part of the fouled membrane.	Overnight at room temperature.	--
N	Neosepta clean.	Overnight at room temperature.	10 μm
NF	Neosepta + fouling	Overnight at room temperature.	10 μm
NFC	Neosepta + fouling + clear	Overnight at room temperature.	10 μm

5.3. INSTRUMENTAL MEASUREMENTS

Measurements of single-point spectra and hyperspectral images were made. In the case of single-point spectra, the samples measured were FuS1, FB, F, FC, NF and N. For the hyperspectral images, the samples used were FuS1, NFC and F. The kind of measurements and the related samples are summarized in table 2.

Table 2. Samples with the measurements done.

Sample code	Membrane	Spectroscopic technique	Measurement mode	Spectral range (cm ⁻¹)	Image	Field of view or pixel size
F	Fujifilm new	Mid-IR	ATR	220-4000	NO	25 x 25 μm ²
FuS1	Fujifilm + fouling	Mid-IR	ATR	220-4000	NO	25 x 25 μm ²
FB	Fujifilm kept in brine	Mid-IR	ATR	220-4000	NO	25 x 25 μm ²
FC	Fujifilm clean part of the fouled membrane.	Mid-IR	ATR	220-4000	NO	25 x 25 μm ²
N	Neosepta clean	Mid-IR	ATR	220-4000	NO	25 x 25 μm ²
NF	Neosepta + fouling	Mid-IR	ATR	220-4000	NO	25 x 25 μm ²
FuS1	Fujifilm + fouling	Mid-IR	Transmission (synchrotron)	600 - 4000	NO	3 x 3 μm ²
NF	Neosepta + fouling	Mid-IR	Transmission (synchrotron)	600 - 4000	NO	3 x 3 μm ²
NFC	Neosepta + fouling + clear	NIR	Reflectance	4000-13000	YES	200 x 200 μm ²
FuS1	Fujifilm + fouling	Mid-IR	Transmission	800 - 4000	YES	25 x 25 μm ²
F	Fujifilm new.	Mid-IR	Transmission	800 - 4000	YES	25 x 25 μm ²

5.3.1. Single-point spectra

The measurements of single-point spectra were made in the Mid-IR spectral range in ATR reflectance mode and transmission mode.

For the single-point ATR-FTIR spectra the instrument used was the PerkinElmer FTIR Frontier located at the Centres Científics i Tecnològics de la UB (CCiTUB). First of all it was necessary to do a background measurement on the CaF₂ slides, afterwards the samples were placed in the instrument and the spectrum was measured. In this case the wavelength range used in the spectra was between 4000-220 cm⁻¹ with a spectral resolution of 4 cm⁻¹ and a spatial field of view of 25 x 25 μm². Spectra were obtained averaging an accumulation of 16 scans per measurement of each sample.

Since this measurement is done in reflectance mode, the part of the sample that is measured is the membrane surface. For that reason, to do the ATR measures the only thing necessary to do with the membranes was to cut them in a tiny circle to do the measurements, any other preparation was not required. The samples measured with ATR were F, FuS1, FB, FC, N and NF.

For the single-point transmission FTIR synchrotron spectra measurements the instrument used was the Hyperion 3000 spectrometer, located at the MIRAS beamline in the ALBA synchrotron installation at Cerdanyola del Vallès. This spectrometer is connected to an IR synchrotron beam source, which allows spatial resolution of 3 x 3 μm², much finer than that provided by a conventional IR light source. To do these measurements the only thing to do was putting the membrane cross-section in the sample compartment and the spectra were obtained picking the zone of interest in the membrane cross-section. The spectral range used was between 4000-400 cm⁻¹. It is important to note that these single-point spectra can be performed on very localized zones of the sample and provide very specific information.

Since this measurement is done in the transmission mode, the samples used were the cross-sections of FuS1 and NF of 10 μm.

5.3.2. Hyperspectral images

The measurements of hyperspectral images were made in Mid-IR, in transmission mode, and in the NIR range, in reflectance mode.

For the Mid-IR hyperspectral images, the Thermo Scientific Nicolet iN10 MX instrument, located at the Centres Científics i Tecnològics de la UB (CCiTUB), was used. First it was necessary to do a measurement of the background on the CaF₂ slide. After that the sample is placed in the instrument and the measurement of the image is done collecting mosaics of 8 x 2 spectra simultaneously and moving the sample in x- and y- directions until all sample surface is scanned. This procedure is controlled using the OMNIC Picta software. The conditions used to do these measurements were a spectral range between 4000-800 cm⁻¹, to avoid the signal of the CaF₂ slides that appears below 800 cm⁻¹, an accumulation of 8 scans per pixel measurement, a spectral resolution of 4 cm⁻¹ and a spatial resolution of 25 x 25 μm².

Since the images are collected in transmission mode, the samples measured were the cross-sections of the membranes F and FuS1 of 10 μm, because thickness is a parameter to keep in mind in this mode.

For the NIR hyperspectral images, the Specim FX17 HSI-NIR instrument located at the Chemometrics laboratory of the Analytical Chemistry section was used. This system is a pushbroom imaging system, which works in line scan mode, collecting a line of pixel spectra simultaneously. To do the measurements of the NIR hyperspectral images, it is necessary to do a reference image to set the 100% of reflectance, called white, one of the 0% of reflectance, called dark and to collect the spectra of the sample of interest. These three measurements are done in the same scanning procedure, the white is measured from a sample of OPRS 200.25.10, which is a high reflectance material, the dark is measured with the camera shutter closed to avoid the light and the sample is imaged afterwards. Both the material used to acquire the white reference and the sample are located in a platform (bed scan) that moves in a longitudinal direction under the NIR camera, see Figure 9. The data acquisition of the sample, the white and the dark were controlled with the Lumo Scanner software. The conditions used to do these measurements were a frame rate of 30 Hz, which is the frequency at which consecutive pixel lines, called frames, are acquired, an exposure time of 3.1 ms, which is the time the detector collects the instrumental response, and a scan speed of 6.5 mm/s, which is the speed at which the bed scan moves.

Since images are collected in reflectance mode the sample did not need any pretreatment, because the measurement is on the membrane surface and the thickness of the sample does not affect the measurements. The sample measured with this mode was the NFC.

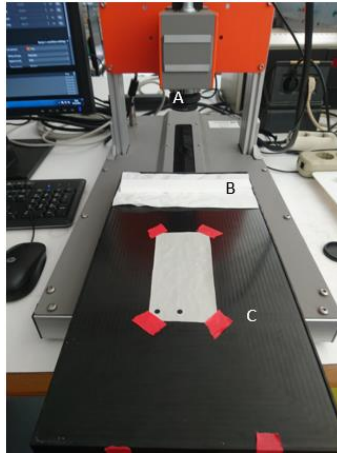


Figure 9. Image of the Specim FX17 HSI-NIR instrument used to make the hyperspectral NIR images.
A: NIR camera; B: White reference; C: Bed scan with a membrane sample.

6. DATA TREATMENT

6.1. SPECTRA PREPROCESSING

In the measurements of single-point spectroscopy by ATR and in transmission mode with FTIR synchrotron, no preprocessing was required and the spectra were interpreted as coming out from the instrument.

The spectra obtained by the NIR imaging system needed a treatment to obtain the absorbance spectra that will be further analysed. First, the data obtained is transformed into a MATLAB file by the HSI-NIR SPECIM converter software.

MATLAB 2018b was used to transform the reflectance data obtained in the NIR measurements to absorbance. To calculate the absorbance, it was necessary to use the white and the dark spectroscopic references measured previously with the instrument, to transform the sample spectra measured. The following equations show the procedure applied.

$$\text{White}_{\text{corrected}} = \text{White}_{\text{rawdata}} - \text{Dark}_{\text{(with same dimension as white)}}$$

$$\text{Sample}_{\text{corrected}} = \text{Sample}_{\text{rawdata}} - \text{Dark}_{\text{(with the same dimension as sample)}}$$

In the procedure of the calculation of the absorbances, it was necessary to eliminate the bad pixels of the spectra related to the white corrected and to the sample corrected. These bad pixels appear because the instrument had some pixels that were not detected appropriately and these could affect the final spectrum obtained. After the bad pixels were eliminated, each reflectance spectrum in the image is obtained before calculating the absorbance spectrum.

$$\text{Reflectance} = \text{Sample}_{\text{withoutbadpixels}} / \text{White}_{\text{corrected}}$$

$$\text{Absorbance} = -\log_{10}(\text{Reflectance})$$

This procedure is the same for all the membrane NIR images measured. Once the absorbances were calculated, it was necessary to do a pretreatment of the data before further data analysis. Two types of pre treatment were tried: the second derivative and the multiplicative scatter correction (MSC) ¹⁵.

The second derivative was used to remove the offset and the linear trend in the baseline. As a negative consequence, it reduces slightly the signal/noise ratio, see figure 10. To do the derivative the Savitzky Golay ¹⁶ method was used, using 15 points window and a second degree polynomial function to fit the data, and with the second degree of the derivative.

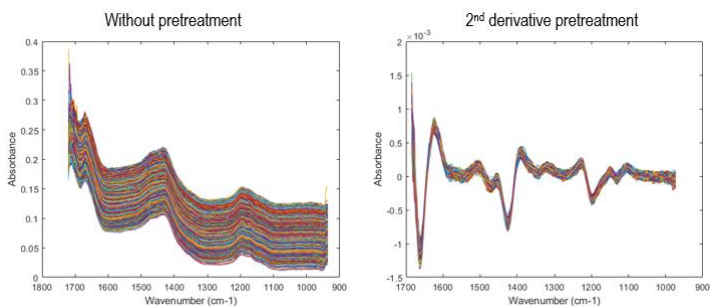


Figure 10. Comparison of NIR spectra without pretreatment on the left, with data treated with 2nd derivative, on the right.

MSC is used to balance the linear baseline present in NIR spectra, produced by the scatter from the particles in the sample, see figure 11. Once finished the baseline correction, the small noisy extremes of the spectra were removed to perform additional data analysis.

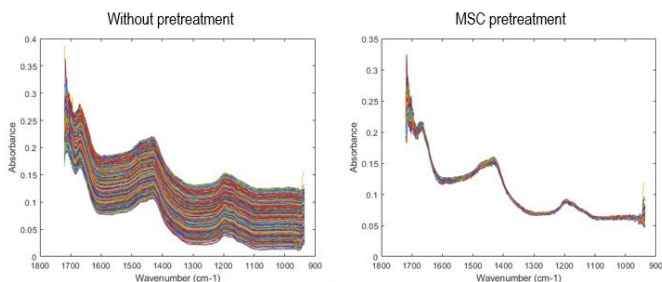


Figure 11. Comparison of NIR spectra without pretreatment on the left, with data treated with MSC, on the right.

The spectra obtained in transmission mode in mid-IR images were baseline corrected using the asymmetric least squares method. The Asymmetric Least Squares (AsLS) ¹⁷ is useful to remove baselines with irregular shapes, see figure 12.

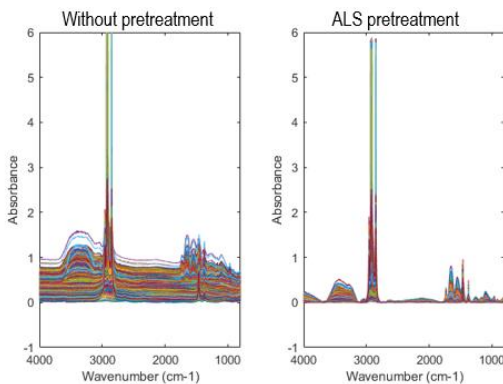


Figure 12. Comparison of data with any pretreatment on the left, with data treated with AsLS, on the right.

6.2. MULTIVARIATE CURVE RESOLUTION-ALTERNATING LEAST SQUARES (MCR-ALS)

MCR-ALS is the method used to analyze the hyperspectral images and to obtain information about the composition of the components of the membranes and the fouling. MCR-ALS is an iterative resolution method that provides the pure spectra and the related distribution maps of the constituents of the sample using the information in the initial image ¹⁸.

In the case of hyperspectral image measurements, the data obtained was the image cube, with all pixel absorbance spectra, see figure 13. All the absorbance spectra of the membrane

are first organized in a data matrix called **D**. All the spectra in matrix **D** can be defined by the equation $\mathbf{D} = \mathbf{C}\mathbf{S}^T$, which corresponds to the expression of the Beer-Lambert law, where all spectra are expressed by the product of the concentration profiles of all compounds (expressed in the **C** columns), by their pure spectra contribution (expressed in the **S^T** rows). This is the bilinear model $\mathbf{D} = \mathbf{C}\mathbf{S}^T + \mathbf{E}$, where **E** is an error matrix.

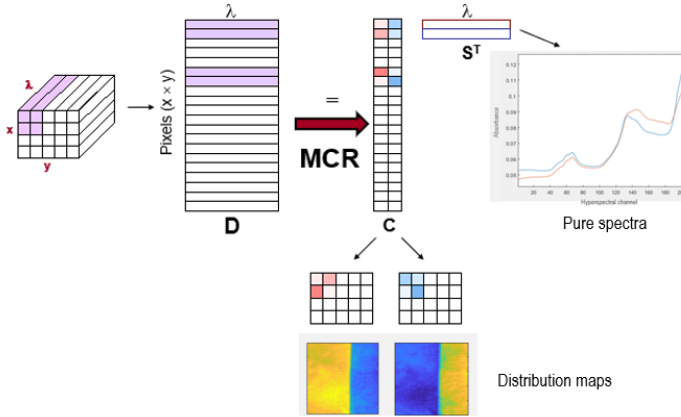


Figure 13. Scheme of use of MCR-ALS applied to analyse a hyperspectral image.

In the measurements of hyperspectral image the only matrix known is **D**, and the pure spectra of all sample compounds and the related concentration profiles are unknown. To solve this problem, the Multivariate Curve Resolution-Alternating Least Squares (MCR-ALS) method can be used. First, it is necessary to find the number of components, *n*, to describe the image by Principal component analysis (PCA) ¹⁹. Second, the *n* most different spectra of the image are provided by a method based on SIMPLISMA ²⁰ and are used as the initial estimate of matrix **S^{T*}**. Having then the row data (**D**) and the initial estimates of **S^{T*}**, the concentration profiles (**C^{*}**) can be calculated by least squares.

$$\mathbf{C}^* = (\mathbf{S}^{T*})^+ \mathbf{D}$$

$$\text{being } (\mathbf{S}^{T*})^+ = \mathbf{S}^* (\mathbf{S}^* \mathbf{S}^{T*})^{-1}$$

After this, **S^{T*}** is recalculated with the new **C^{*}** by least-squares.

$$\mathbf{S}^{T*} = \mathbf{D}\mathbf{C}^{*+}$$

$$\text{being } \mathbf{C}^{*+} = \mathbf{C}^* (\mathbf{C}^* \mathbf{C}^{*+})^{-1}$$

Having **C^{*}** and **S^{T*}** the matrix **D^{*}** can be calculated using these new estimates.

$$\mathbf{D}^* = \mathbf{C}^* \mathbf{S}^{T*}$$

Immediately \mathbf{D}^* is compared to the original matrix, \mathbf{D} . The iterative optimization is finished when the difference between \mathbf{D}^* and \mathbf{D} is sufficiently small. The convergence criterion to consider small the difference between \mathbf{D}^* and \mathbf{D} was 0.1% for the difference of the lack of fit (LOF) between two consecutive iterations. The lack of fit and the variance explained are two parameters used to evaluate the quality of the model fit.

$$\text{Lof}(\%) = 100 \times \sqrt{\frac{\sum_{ij} e_{ij}^2}{\sum_{ij} d_{ij}^2}}$$

$$r^2(\%) = 100 \times \left(1 - \frac{\sum_{ij} e_{ij}^2}{\sum_{ij} d_{ij}^2} \right)$$

Where d_{ij} is the original element of \mathbf{D} and e_{ij} is the related residual value obtained from the difference between \mathbf{D} and \mathbf{D}^* obtained from MCR-ALS, of the row i and the column j .

For the calculation of \mathbf{C}^* and \mathbf{S}^{T*} different constraints can be applied. In the case of the membranes, the constraint applied was the non-negativity in the spectra and in the concentration profiles, because none of them can have negative values in our case. Last of all, the distribution maps of each component in the image were obtained refolding each concentration profile according to the original spatial structure of the image, see figure 13.

Sometimes different images need to be treated together to obtain more easily all the necessary information of the sample. In this case it is necessary to build what is known as a multiset, see figure 14, connecting the block of spectra of the different images one under the other. In this case, MCR-ALS provides a single matrix with the pure spectra of the components in all images and an augmented matrix \mathbf{C} with blocks related to each image in the multiset. Distribution maps of each image are obtained. In this work in the case of the Fujifilm membrane, a multiset formed by the spectra of the new Fujifilm membrane (F) and the fouled Fujifilm membrane (FuS1) will be analysed. In the case of the multisets sometimes is possible to know which component belong to each image, as the case of the component of the fouling that only belongs to the data of the fouled membrane. This information is used as a constraint called correspondence of species to do the MCR analysis with the non-negativity of the spectra and the concentration profiles.

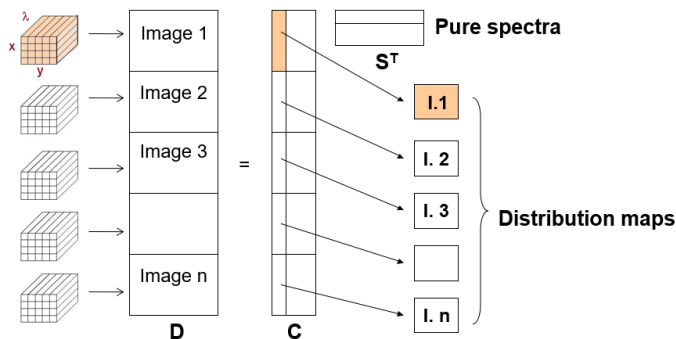


Figure 14. Representation of the MCR-ALS analysis of a multiset of a matrix D with n hyperspectral images.

The method MCR-ALS has been applied using a graphical user interface working under MATLAB18a²¹.

7. RESULTS AND DISCUSSION

7.1. OPTICAL CHARACTERIZATION OF MEMBRANES

The samples measured were the membranes without pretreatment in reflectance mode, and the cuts of the membrane cross-sections embedded in paraffin in transmission mode, see figure 15. The brown fouling of the Fujifilm membrane comes from the wine production and may be formed mainly by polyphenols and polysaccharides. The cross-section of the Fujifilm membrane shows disordered nanofibers made by the electrospinning process of membrane manufacturing¹. The brown film above the cross-section is due to the fouling. The pink fouling of Neosepta may be formed by molecular sulphur coming from the use of the membrane for the valorisation of acidic liquid wastes. The cross-section of the membrane shows the ordered fibres of the PVC fabric, which is the base of the Neosepta membrane.

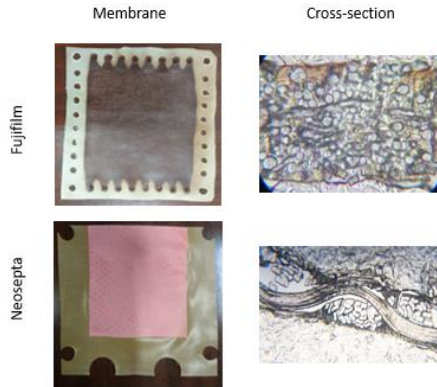


Figure 15. Image of the membranes measured (Fujifilm, top plots; Neosepta, bottom plots). On the left, intact membranes to measure the surface by reflection mode; on the right, cross-sections of membranes to be measured in transmission mode.

For the Fujifilm membrane there were three different ways to dry the samples. At first sight looking at the figure 16, there is no difference between the three treatments, previously explained in section 5, because in all of them seems that the sample was embedded in the right way preserving the fouling and the membrane structure without any visible difference. Since no appreciable differences are found among the different drying treatments, measurements will be done on the membranes without any treatment to preserve the samples as unaltered as possible.



Figure 16. Cross-sections of the Fujifilm with fouling membrane dried with different treatments.

The difference between the clean membrane and the fouled one embedded in paraffin for both Fujifilm and Neosepta membranes is that the fouled ones have a surface with different colour. In the case of the Fujifilm the fouled part was brown and the difference between new and fouled membrane is easy to see looking at figure 17.

In the case of the Neosepta membrane looking at figure 17 it is possible to see that the fouled part is pink, but the difference of colour is not that easy to see as in the case of the Fujifilm membrane.

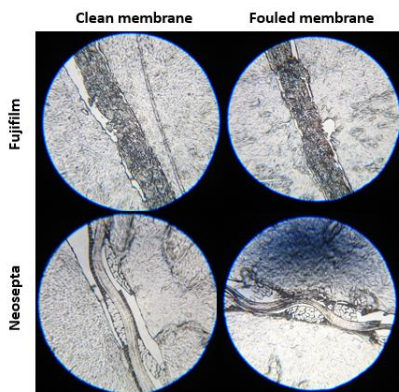


Figure 17. Comparison between the clear membrane and the fouled membrane of the two types studied.

7.2. SINGLE-POINT SPECTROSCOPY OF MEMBRANES

The measurements done with ATR, in reflectance mode, are done on the surface of the sample and with the membranes without any pretreatment.

In the case of the Fujifilm spectra for the two new membranes, F and FB, there are differences according to the way that they were kept, see figure 18A. At 1331 cm^{-1} there is a big band in the new membrane that the membrane kept in brine does not have, but it could not be defined the related compound. It seems that this compound could be washed out from the new membranes when they are put in a brine solution.

Between the fouled membrane (FuS1) and the new one kept in brine (FB) there are subtle differences, the main one that is possible to see is that the bands of the amides²², the active group of the membrane that appears between $1250 - 1700\text{ cm}^{-1}$, are less intense in the fouled. Another difference is that in the peak at 1726 cm^{-1} , which corresponds to the C-O band, the intensity in the fouled membrane seems lower as well. The shape of the band above 3000 cm^{-1} also changes due possibly to the presence of polyphenols in the wine fouling that give signal in this spectral region, see figure 18B.

A big difference could be seen between the fouled part (FuS1) and the clean part (FC) in the Fujifilm membrane used in the wine process because the clean part has three bands very different in the range of 700-1300 cm^{-1} . These bands correspond to silicone, the one in 800 cm^{-1} corresponds to Si-CH₃, the middle one between 1020-1100 cm^{-1} correspond to Si-O-Si and the last one at 1260 cm^{-1} to Si-(CH₃)₂, see figure 18C. These bands can come from residues of the membrane separators in the wine process.

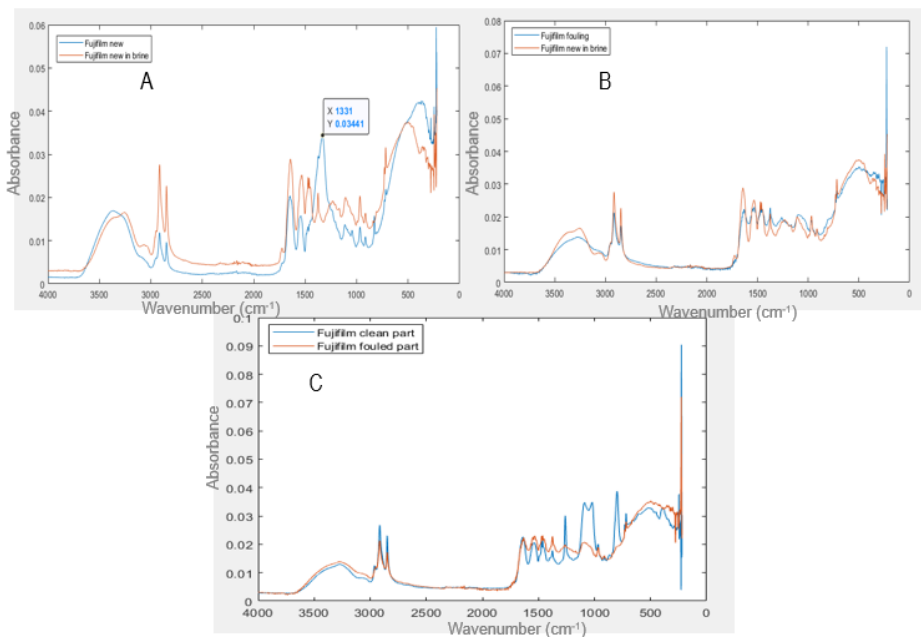


Figure 18. A: Spectra of F and FB. B: spectra of FB and FuS1. C: spectra of FC and FuS1.

In the case of the Neosepta membrane, the characterization of the fouling was not conclusive because the spectra obtained by ATR showed almost no signal. That happened probably because the component of the surface, possibly molecular sulphur, does not give a significant signal, see figure 19.

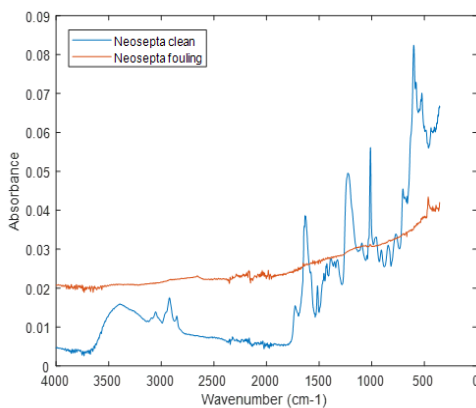


Figure 19. Spectra of the fouled (NF) and the clean (N) part of the Neosepta membrane.

To have better spectra in specific and localized zones of the membranes, measurements in transmission mode with FTIR synchrotron spectroscopy were done on the cross-sections of the fouled Fujifilm membrane and the fouled Neosepta membrane.

In the case of the Fujifilm membrane two spectra were measured, one of the cross fibres (A) and another one of the fouled part (B). As it can be seen in figure 20, the spectra are very different due to the difference in composition of the fibres and the fouled part. This difference can be seen because the spatial resolution of the synchrotron ($3\ \mu\text{m}$) is better than that the FT-IR conventional images ($25\ \mu\text{m}$) and spectra can be associated with very specific zones of the membrane. The spectrum A corresponds to the polyolefin of the fibres as shown with the bands in the region of $1300\text{-}1500\ \text{cm}^{-1}$, typical of this functional group, and the spectrum B to the polyphenol and the polysaccharides of the fouling, in the zone above 3000cm^{-1} , and the polyamide matrix, seen in the region between $1400\text{-}1700\ \text{cm}^{-1}$.

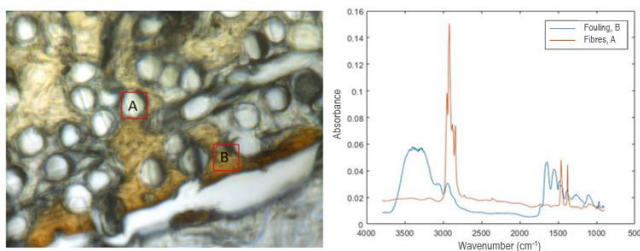


Figure 20. Image of the cross section of a Fujifilm membrane with fouling on the left. Spectra of the points measured of the membrane on the right.

In the case of the Neosepta membrane, the fouled membrane embedded in paraffin was measured. The spectra were one of the longitudinal fibres (C), and the other one on the transversal part of the fibres that may include some fouling (D). Looking at the two spectra together, in figure 21, it is possible to see that both are very similar and there are no significant spectral differences between the two points of the membrane.

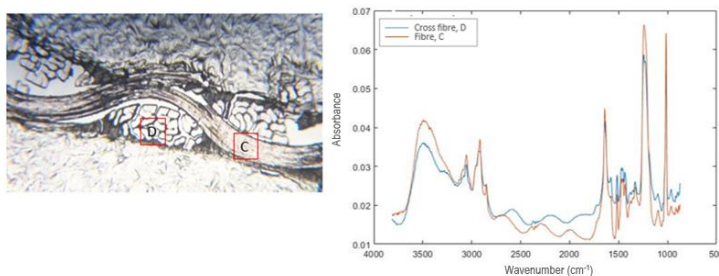


Figure 21. Image of the cross section of a Neosepta membrane with fouling on the left. Spectra of the points measured of the membrane on the right.

7.3. HYPERSPECTRAL IMAGES

Hyperspectral images were measured in two different modes, in transmission mode in the Mid-IR range and in reflectance mode for the NIR range.

7.3.1. Mid-IR images

The only images analysed in transmission mode were the ones that correspond to the cross-sections of the Fujifilm membrane because this membrane showed more differences among components using FT-IR spectroscopy. The samples used were cross-sections of 10 μm of thickness, and an area of a few squared millimetres.

A multiset, formed by the spectra of the images of the new Fujifilm membrane and the fouled Fujifilm membrane one under the other as shown in Figure 22, was analysed. Both images come from samples embedded in paraffin. The MCR model gives in this case a single matrix \mathbf{S}^T with the pure spectra of the components present in the membranes and an augmented \mathbf{C} matrix, from which maps for all components related to the clean Fujifilm membrane and to the fouled membrane can be derived.

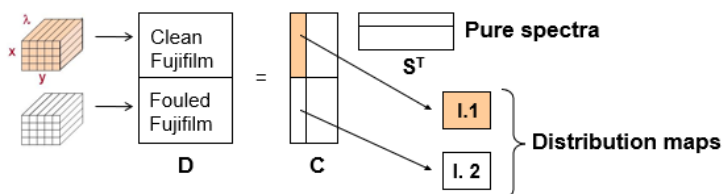


Figure 22. Multiset used in the MCR-ALS method.

In the MCR results, it is possible to see that the Fujifilm membrane has four components, see figures 23 and 24, and the percent of variance explained by the MCR model was 99.10. The constraints applied were non-negativity in the concentration and pure spectra and correspondence of species, setting that the clean membrane should not have the component related to fouling.

The first component corresponds to the paraffin that was the embedding medium where the sample is. In the pure spectrum, the characteristic bands of the paraffin were shown at 1400-1500 cm^{-1} , see figure 24A. The distribution map shows clearly that the paraffin is surrounding the membrane cross-section, see figure 23A.

The second component corresponds to the polyamide matrix of the membrane. The pure spectrum shows the bands of amides, in the region between 1400-1700 cm^{-1} , and a band at the region between 3100-3600 cm^{-1} , which agrees with the spectrum of the synchrotron on a point where fouling and polyamide matrix are present, see figure 24B. The map of this component is in the membrane in discontinuous zones, see figure 23B.

The third component corresponds to the membrane fibres, formed by polyolefin components, as shown in the bands in the region of 1300-1500 cm^{-1} . This component shows the same bands as the spectra obtained in the single-point measurements in transmission mode of the fibres in the synchrotron, see figure 24C. The map of this component shows a big density inside the membrane because the fibres are the major compound of the membrane, see figure 23C.

The last component corresponds to the fouling and, as set by the correspondence of species constraint, see figure 23D, is not present in the image of the clean membrane. In the spectra the bands in the region between 900-1200 and around 1600 cm^{-1} corresponds to polysaccharides that are present in the wine. The band in the 3500-3600 cm^{-1} can be from the polyphenols compounds, which extraction is in an important procedure in the wine ²³, see figure 24D.

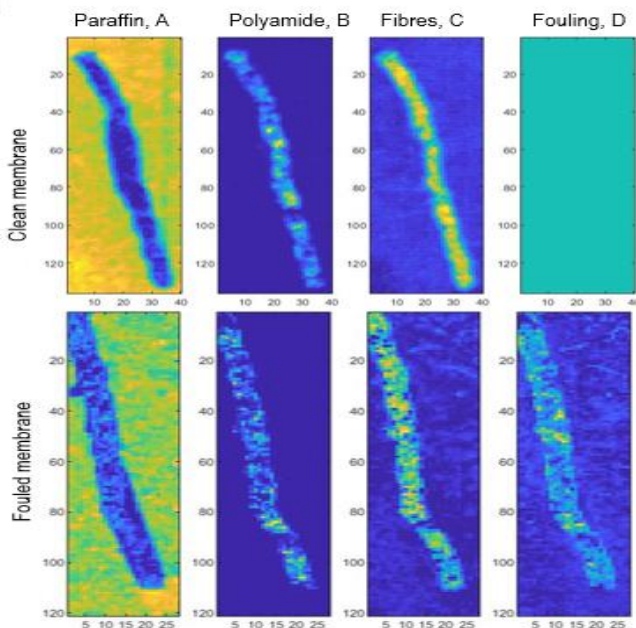


Figure 23. Distribution maps after applying the MCR-ALS method.

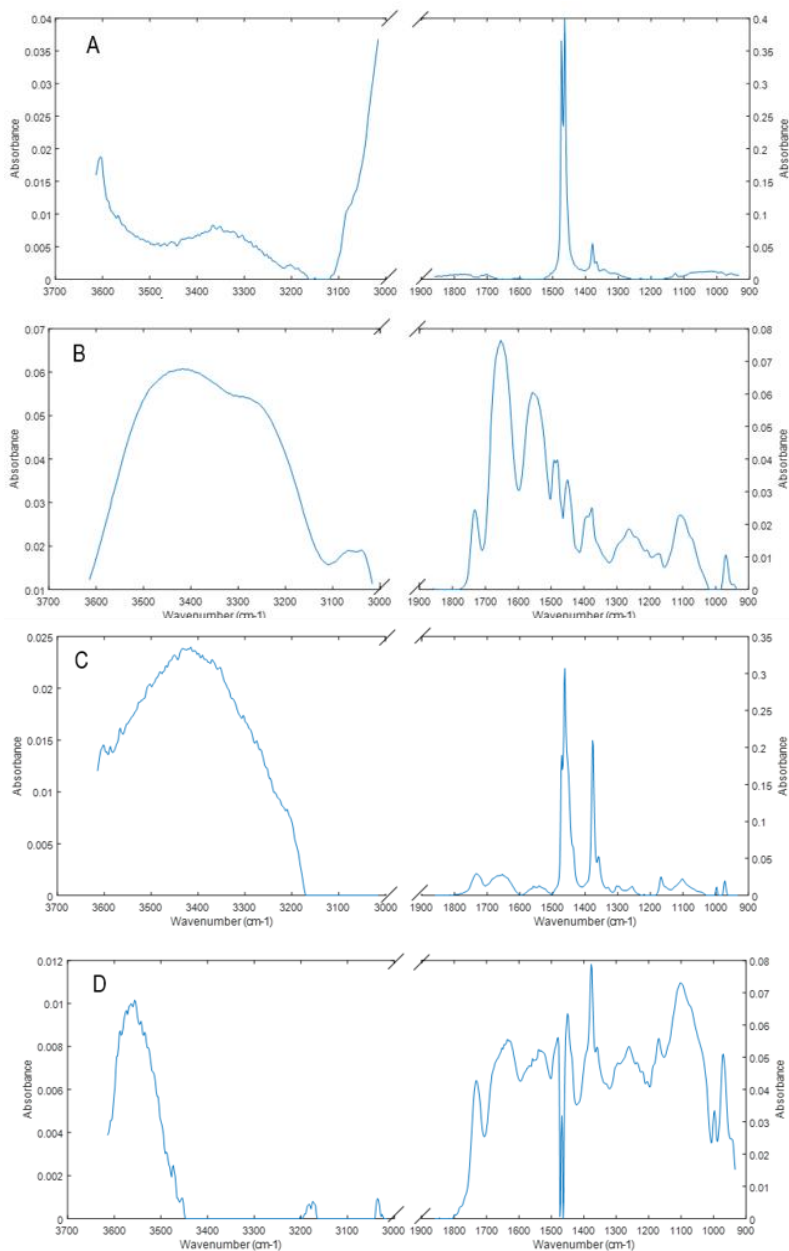


Figure 24. Spectra of the four components found with the MCR-ALS. A: paraffin. B: polyamide. C: fibres. D: fouling.

7.3.2. NIR hyperspectral images

The spectra of NIR images obtained in both Fujifilm and Neosepta membranes were preprocessed to see if the spectra of the fouled part and the clean part showed different shapes. All images collected had a pixel size of $200 \times 200 \mu\text{m}^2$, and a 60×60 pixels, which means that the surface measured for each image was $1.2 \times 1.2 \text{ cm}^2$. Baseline correction with MSC or 2^{nd} derivative was done to appreciate better the differences between fouling and clean membrane.

In the case of the Fujifilm membrane neither MSC nor 2^{nd} derivative showed any difference between the fouled and the new membrane, see figure 25. That made impossible to do a characterization of the membrane based on NIR images because it could not be possible to differentiate the component that corresponds to the fouling and the component that correspond to the new membrane.

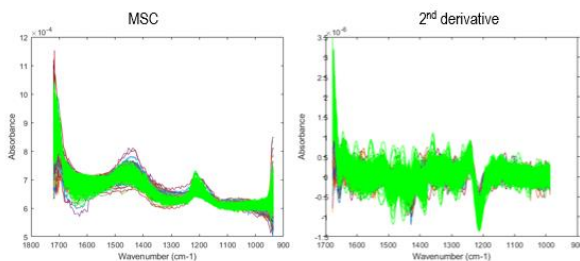


Figure 25. In green the spectra of the fouling of the Fujifilm membrane after baseline correction with MSC or the 2^{nd} derivative. The spectra in different colours correspond to the new Fujifilm membrane treated after baseline correction with MSC or the 2^{nd} derivative.

In the case of the Neosepta membrane the comparison between the spectra of the clean part (N) and the fouled part (NFC) after baseline correction with MSC showed difference in the spectral bands obtained, see figure 26. That made possible to do the characterization of the membrane with MCR, characterizing and locating different components has the membrane.

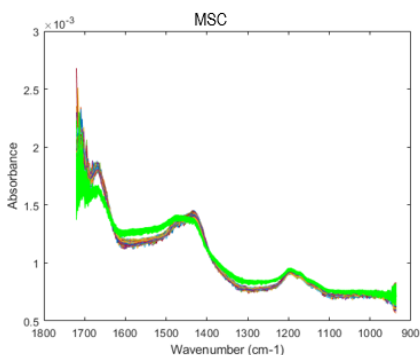


Figure 26. In green the data of the clean Neosepta membrane, the rest of the data corresponds to the fouling part of the Neosepta membrane. All the data was treated with MSC.

After the treatment of MSC that showed differences between the fouled and the clear part, MCR analysis in the border zone of the NFC sample where at simple sight fouling and clean part are present was done. MCR analysis resolved two components and the percent of variance explained by the MCR model was 99.99. No better results were obtained if additional components were proposed in the MCR analysis. The MCR-ALS analysis resolved two different components, one that belonged to the fouled part and the other to the clean part. That can be seen in figure 27, where on the left are the two different distribution maps of the components of the hyperspectral image and, on the right, the related pure spectra.

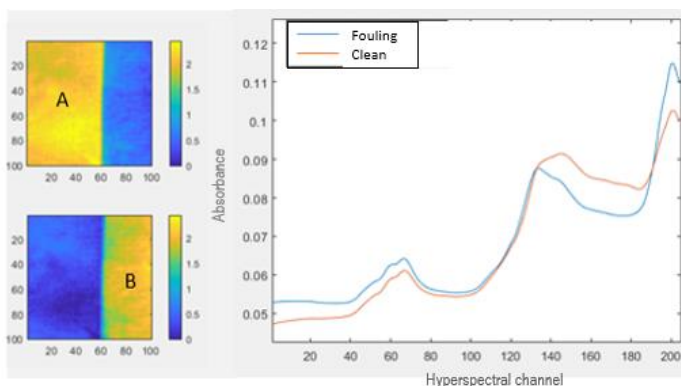


Figure 27. MCR results of the analysis of the NIR image of the Neosepta membrane. On the left, distribution maps of A: fouling, B: clean membrane are seen. On the right, the two pure spectra of each component are displayed.

8. CONCLUSIONS

1. As the main conclusion, the use of hyperspectral images and multivariate resolution methods seems promising to study the identity and spatial distribution of the fouling and structural compounds of industrial membranes. Below, conclusions on specific aspects of this study are described.

2. **On the sample treatment.** No differences between the drying methods tested were seen in the membrane structure or fouling, which means that the best way to work with the membranes is avoiding any treatment to preserve as well as possible the characteristics of the membrane and the fouling.

2. **On the use of single-point spectroscopy.:**

- To characterize the surface of the membranes, the reflectance mode (ATR) in the Mid-IR, can be proposed.
- To characterize the membrane structure and the fouling, it is necessary to do the measurements of the cross-sections in transmission mode. If it is possible, the best method to do the characterization is with the FTIR synchrotron spectra because it has more spatial resolution and specific small points of the membrane can be adequately scanned.
- For the two membranes, a characterization with the FTIR synchrotron spectra was possible. In the Neosepta membrane, the spectra of the fibres could be found and no clear fouling signal could be distinguished. For the Fujifilm membrane, the spectra of the fouling and the spectra of the fibres were differentiated. Moreover, the differences in the Fujifilm membrane surface with and without fouling could be characterized in reflectance mode.

3. **On the hyperspectral images.** This method was used to determine the composition of the membranes and the fouling and the spatial distribution of the different components.

- NIR images in reflectance mode are proposed to identify the composition of the surface of the membrane, although the spatial resolution is not very high (around 200 x 200 μm^2). These images are fast and membranes do not require any sample treatment.

- The Mid-IR images are apt to study the membrane cross-section to characterize the composition of the membrane and the composition of the fouling. The spatial resolution is better (around $25 \times 25 \mu\text{m}^2$), but the preparation of the cross-section needs to be careful and with a small thickness. Still, not all membrane components can be defined perfectly from a spatial point of view.
- With the help of the MCR-ALS method to treat the images, it was possible, in the case of the Neosepta membrane to characterize the surface with NIR imaging and find the component that corresponds to the membrane and the one that correspond to the fouling of the surface of the membrane. For the Fujifilm membrane, the characterization was possible with Mid-IR images. In this case four components were found, one for paraffin, the media were the sample was, two for the composition of the membrane, related to fibres and polyamide material, and one for the wine fouling, with some bands of polyphenols and polysaccharides.

4. **Future work.** The problems solved in this study about sample treatment and image interpretation will be useful in the future, where hyperspectral image measurements will be done with FT-IR synchrotron imaging to characterize with more detail the spatial composition of the membranes and their fouling.

9. REFERENCES AND NOTES

1. Sarapulova, V.; Shkorkina, I.; Mareev, S.; Pismenskaya, N.; Kononenko, N.; Larchet, C.; Dammak, L.; Nikonenko, V. Transport Characteristics of Fujifilm Ion-Exchange Membranes as Compared to Homogeneous Membranes AMX and CMX and to heterogeneous Membranes MK-40 and MK-41. *MDPI, Membranes* **2019**.
2. Ran, J.; Wu, L.; He, Y.; Yang, Z.; Wang, Y.; Jiang, C.; Ge, L.; Bakangura, E.; Xu, T. Ion exchange membranes: New developments and applications. *Journal of Membrane Science*, Elsevier. **2016**.
3. Blanco, M.; Coello, J.; Iturriaga, H.; Maspocho, S.; de la Pezuela, C. Near-infrared spectroscopy in the pharmaceutical industry. *The analyst*, Vol. 123 (135R-150R), **1998**.
4. Bellon-Maurel, V.; McBratney, A. Near-infrared (NIR) and mid-infrared (MIR) spectroscopic techniques for assessing the amount of carbon stock in soils – Critical review and research perspectives. *Soil Biology & Biochemistry*, Elsevier. **2011**.
5. Perkinelmer, technical note, FT-IR Spectroscopy. Attenuated Total Reflectance (ATR). https://cmds.rpi.edu/sites/default/files/ATR_FTIR.pdf (accessed **January 2020**).
6. Técnicas de muestreo FTIR: transmisión. <https://www.thermofisher.com/es/es/home/industrial/spectroscopy-elemental-isotope-analysis/spectroscopy-elemental-isotope-analysis-learning-center/molecular-spectroscopy-information/ftir-information/ftir-sample-handling-techniques/ftir-sample-handling-techniques-transmission.html> (accessed **January 2020**).
7. Larkin, P. J. *Infrared and Raman Spectroscopy (Second Edition)*. Chapter 3 – Instrumentation and Sampling Methods, pages 29-61. **2018**.
8. Armenta, S.; de la Guardia, M. *Comprehensive Analytical Chemistry*, Volume 57. Chapter 4 – Avoiding Sample Treatments. **2011**.
9. IUPAC. *Compendium of Chemical Terminology*, 2nd ed. (the "Gold Book"). Compiled by A. D. McNaught and A. Wilkinson. Blackwell Scientific Publications, Oxford (1997). Online version (2019-) created by S. J. Chalk. ISBN 0-9678550-9-8.
10. Ion exchange membranes for water purification, Fujifilm membrane technology. https://www.fujifilmmembranes.com/images/Fujifilm_IEM_product_version_1.2_publish_website.pdf (accessed **January 2020**).
11. El Rayess, Youssef and Mietton-Peuchot, Martine. Membrane Technologies in Wine Industry: An Overview. (2016) *Critical Reviews in Food Science and Nutrition*, 56 (12). 2005-2020. ISSN 1040-8398).
12. Comparison table for detailed specification of Cation/Anion Exchange Membrane from <http://www.astom-corp.jp/en/product/10.html> (accessed **January 2020**).
13. PhD tesis of Julio López Rodríguez. Integration of Nanofiltration and Diffusion Dialysis for the sustainable management of acidic liquid wastes. December **2019**.
14. Xie, M.; Luo, W.; Gray, S. R. Synchrotron Fourier transform infrared mapping: A novel approach for membrane fouling characterization. *Water Research*, Elsevier. **2017**.
15. Geladi, P.; McDougall D.; Martens, H. Linearization and Scatter-Correction for Near-Infrared Reflectance Spectra of Meat. Vol. 39. No. 3. **1985**.
16. Savitzky, A.; Golay, Mje. Smoothing + differentiation of data by simplified least squares procedures. *Analytical Chemistry*. Volume: 36 Issue: 8. **1964**.
17. Paul H. C. Eilers. Parametric Time Warping. *Analytical Chemistry*, Vol. 76, No. 2. **2004**.
18. De Juan, A; Jaumot, J; Tauler, R. Multivariate Curve Resolution (MCR). Solving the mixture analysis problem. *Analytical Methods*, Vol. 6, No 14, p. 4964-4976. **2014**.
19. Jolliffe, I. *Principal component analysis*. Springer Berlin Heidelberg. **2011**.
20. Windig, W., & Guilment, J. Interactive self-modeling mixture analysis. *Analytical chemistry*, 63(14), 1425-1432. **1991**.

21. Jaumot, J., de Juan, A., & Tauler, R. MCR-ALS GUI 2.0: new features and applications. *Chemometrics and Intelligent Laboratory Systems*, 140, 1-12. **2015**.
22. Yurkanis Bruice, P.; Química Orgánica (Quinta Edición). Apéndice VI, pages A-21 – A-23. Table. Frecuencias en el infrarojo características de grupo. **2008**.
23. Olejar, K. J.; Ricci, A.; Swift, S.; Zujovic, Z.; Gordon, K. C.; Fedrizzi, B.; Versari, A.; Kilmartin, P. A. Characterization of an Antimicrobial Extract from Cool Climate, White Grape Marc. MDPI, Antioxidants. **2019**.

